


ORIGINAL ARTICLE

Downregulation of miRNA-26 in chronic periodontitis interferes with innate immune responses and cell migration by targeting phospholipase C beta 1

Juhi R. Uttamani¹ | Afsar R. Naqvi² | Araceli Maria Valverde Estepa² |
Varun Kulkarni² | Maria F. Brambila³ | Gloria Martínez³ | Gabriela Chapa³ |
Christine D. Wu⁴ | Wei Li⁴ | Sona Rivas-Tumanyan⁵ | Salvador Nares² 

¹Department of Periodontics, College of Dentistry and Dental Clinics, University of Iowa, Iowa City, Iowa, USA

²Department of Periodontics, College of Dentistry, University of Illinois Chicago, Chicago, Illinois, USA

³Posgrado de Periodoncia, Facultad de Odontología, Universidad Autónoma de Nuevo León, Monterrey, Mexico

⁴Department of Pediatric Dentistry, College of Dentistry, University of Illinois at Chicago, Chicago, Illinois, USA

⁵Office of Assistant Dean for Research and Department of Surgical Sciences, University of Puerto Rico School of Dental Medicine, San Juan, Puerto Rico

Correspondence

Salvador Nares, Department of Periodontics, College of Dentistry, University of Illinois at Chicago, 458 Dent MC 859, 801 South Paulina Street, Chicago, IL 60612, USA.
Email: snares@uic.edu

Funding information

National Institutes of Health, Grant/Award Numbers: DE021052 (SN), DE026259 (ARN), DE027980 (ARN); University of Illinois at Chicago

Abstract

Aim: To evaluate the potential role of miR-26 family members in periodontal pathogenesis by assessing innate immune responses to periopathic bacteria and regulation of cytoskeletal organization.

Materials and Methods: Expression of miR-26a-5p and miR-26b-5p was quantified in gingival biopsies derived from healthy and periodontally diseased subjects before and after non-surgical (scaling and root planing) therapy by RT-qPCR. Global pathway analysis and luciferase assays were performed for target identification and validation. Cytokine expression was assessed in miR-26a-5p transfected human oral keratinocytes upon stimulation with either live *Porphyromonas gingivalis* (Pg), *Aggregatibacter actinomycetemcomitans* or Pg lipopolysaccharide (LPS). Wound closure assays were performed in cells transfected with miR-26a-5p, while the impact on cytoskeletal organization was assessed by F-actin staining.

Results: miR-26a-5p and miR-26b-5p were downregulated in diseased gingiva and restored 4–6 weeks post-therapy to levels comparable with healthy subjects. Target validation assays identified phospholipase C beta 1 as a bona fide novel target exhibiting antagonistic expression pattern in disease and post-therapy cohorts. miR-26a-5p transfected cells secreted higher levels of cytokine/chemokines upon stimulation with periopathogens and demonstrated impaired cell migration and cytoskeletal rearrangement.

Conclusions: Downregulated miR-26a-5p levels in periodontal inflammation may interfere with key cellular functions that may have significant implications for host defence and wound healing.

KEYWORDS

cell migration, cytoskeleton, microRNA, periodontitis, phospholipase C

Juhi R. Uttamani and Afsar R. Naqvi contributed equally to this study.

This is an open access article under the terms of the [Creative Commons Attribution-NonCommercial-NoDerivs](https://creativecommons.org/licenses/by-nc-nd/4.0/) License, which permits use and distribution in any medium, provided the original work is properly cited, the use is non-commercial and no modifications or adaptations are made.

© 2022 The Authors. *Journal of Clinical Periodontology* published by John Wiley & Sons Ltd.

Clinical Relevance

Scientific rationale for study: We compared miR-26 (-26a-5p and -26b-5p) expression in gingival biopsies from periodontally healthy and diseased subjects before and after non-surgical therapy and correlated the outcomes with the pathophysiology of periodontal disease.

Principal findings: Downregulation of miR-26 expression in periodontal disease was restored to levels observed in healthy gingiva after non-surgical periodontal therapy. Mechanistically, miR-26a-5p modulates inflammation, cell migration and cytoskeleton arrangements of oral keratinocytes and PDL fibroblasts via direct interaction with phospholipase C beta 1.

Practical implications: Epigenetic re-programming by disease-associated microRNAs can regulate periodontal inflammation and its resolution, and provide emerging insights for diagnostic molecular tools.

1 | INTRODUCTION

MicroRNAs (miRNAs) participate in the RNA interference mechanism to regulate post-transcriptional gene expression, thus playing an instrumental role in multiple physiological and pathophysiologic functions (Guil & Esteller, 2009; O'Connell et al., 2010). The mature miRNA-guided protein machinery associates with transcripts and affects target structural stability or interferes with translation (Kulkarni et al., 2016). Immune-mediated diseases, including periodontitis, cause persistent inflammation and tissue destruction of target sites, while other sites remain unaffected, indicating a differential response to bacteria, differences in microbiome or changes in the regulation of inflammatory genes (Offenbacher et al., 2008). A possible explanation could be the epigenetic programming occurring locally at the biofilm–gingival interface leading to changes between inflamed (diseased) versus non-inflamed (healthy) sites (Seo et al., 2015). Because miRNAs are involved in controlling components of the epigenetic machinery, it is crucial to assess their role in the mechanisms associated with periodontal inflammation and in the pathophysiology of periodontal disease.

To explain the molecular mechanisms associated with periodontitis, numerous investigators, including our lab, have compared miRNA expression profiles of diseased and healthy periodontal tissues (Perrì et al., 2012; Stoecklin-Wasmer et al., 2012; Naqvi et al., 2014, 2018a, 2018b, 2019). Our work on cataloguing miRNAs in human inflamed gingival biopsies, derived from an independent cohort of subjects, found miR-26a-5p to be differentially expressed (Naqvi et al., 2019). Additionally, data derived from a follow-up study performed on gingival biopsies from a second, geographically distinct cohort of periodontitis subjects, identified downregulated expression of miR-26a-5p and miR-26b-5p correlating with the pathophysiology of periodontitis. However, its role in periodontal inflammation/resolution and regulatory functions is largely unknown.

The aim of this study was to elucidate the underlying biological consequences of the downregulated expression of miR-26a-5p and miR-26b-5p observed in our clinical samples. The persistent inflammatory response and associated changes in cellular content

observed in periodontitis are key factors that contribute to disease progression. Hence, we evaluated the potential role of miR-26a-5p in periopathogen-induced immune responses, cell migration and cytoskeletal rearrangement in human oral keratinocytes (HOK) and PDL-F (periodontal ligament) fibroblasts, two key cell types of the periodontium.

2 | MATERIALS AND METHODS**2.1 | Study population and sample collection**

This study was conducted in accordance with the Declaration of Helsinki and approved by the Ethics Committee at the University Autónoma de Nuevo León, Facultad de Odontología de Nuevo León, Monterrey, Mexico, and at the University of Illinois, Chicago, College of Dentistry, Chicago, IL. The study population consisted of 54 systemically healthy, non-smoking subjects from two geographically distinct cohorts. Cohort 1 consisted of $N = 15$ periodontitis and $N = 15$ healthy control subjects presenting to the Postgraduate Periodontics Clinic at the Universidad Autónoma de Nuevo León. Cohort 2 consisted of $N = 12$ periodontitis and $N = 12$ healthy control subjects presenting to the Postgraduate Periodontics Clinic at the University of Illinois, Chicago. The inclusion and exclusion criteria and clinical parameters are described in Supplemental Materials and Methods. Briefly, subjects demonstrating at least four teeth with periodontal probing depths (PPD) ≥ 6 mm, clinical attachment loss ≥ 5 mm, bleeding on probing (BOP) and radiographic evidence of bone loss were classified as Stage III, Grade B periodontitis (Tonetti et al., 2018) and were included in the periodontitis group. Healthy controls displayed probing depths ≤ 3 mm, no evidence of attachment loss, no BOP and no radiographic evidence of bone loss. Pre- and post-therapy (scaling and root planing) gingival biopsy samples were collected from Cohort 2. The post-therapy sample was collected after 4–6 weeks from a site distinct from the first biopsy site. The gingival biopsy samples were washed with sterile phosphate-buffered saline, immediately placed in RNAlater solution (Qiagen, Gaithersburg, MD) and stored at -80°C until further use.

2.2 | Total RNA isolation, cDNA synthesis and quantitative real-time PCR

Tissue samples were lysed using the TissueLyzer (Qiagen) and total RNA isolated using the miRNeasy kit (Qiagen), with subsequent miRNA and mRNA expression analysis as previously reported (Perri et al., 2012; Naqvi et al., 2019) and detailed in Supplemental Materials and Methods.

2.3 | miRNA targeted pathway and gene prediction analysis

We selected DIANA-microT-CDS algorithm, which included predicted miRNA targets (Paraskevopoulou et al., 2013). To identify the potential miRNA binding sites on miR-26a regulated genes, miRwalk (<http://mirwalk.umm.uni-heidelberg.de/>) prediction tool was used. We selected eight different algorithm tools (DIANAmT, miRanda, miRDB, miRWalk, PICTAR5, PITA, RNA22 and Targetscan) to identify potential targets.

2.4 | Luciferase reporter constructs and dual luciferase reporter assays

Cloning of predicted gene 3' untranslated region (UTR) and dual luciferase assays were performed as previously described (Naqvi et al., 2015). The 3'UTR of phospholipase C beta 1 (PLCB1) was cloned using Phusion Taq polymerase (NEB, Ipswich, MA) and primers (forward: GCACTCGAGCAGAAGCCAGATGCTCACAA; reverse: ATGCCGCCGCGGAAGAAACATCATGCCA) and is detailed in Supplemental Materials and Methods.

2.5 | Cell culture and transient miRNA transfections

Cell culture conditions are described in Supplemental Materials and Methods. Transient transfections were performed using miScript miR-26a-5p mimetic, inhibitor or control (Qiagen) or at 20 or 50 nM and Lipofectamine 2000 (Life Technologies, Carlsbad, CA) in human embryonic kidney (HEK293), HOK, PDL-F and HeLa cells as previously described (Naqvi et al., 2018a, 2018b). Red siGLO oligos (ThermoScientific) were used as transfection controls for every experiment. Transfection efficiency data are shown in Figure S1.

2.6 | Expression of miR-26a-5p and PLCB1 in a murine model of ligature-induced periodontitis

Periodontitis was induced using a 6-0 silk ligature placed bilaterally between the maxillary first and second molar and local injection of *Porphyromonas gingivalis* (Pg) strain W83 (2 µl of 1×10^9 pfu) around

buccal and palatal gingiva in 8-12-week-old female mice ($n = 6$) under anaesthesia for 4 and 8 days (detailed in Supplemental Materials and Methods).

2.7 | Cytokine analysis

HOK cultures were challenged with live *Pg. Aggregatibacter actinomycetemcomitans* (Aa) strain Y4 (serotype B) at 50, 100 and 250 multiplicity of infection (MOI) or 100 ng/ml *Pg* lipopolysaccharide (LPS) (Sigma Aldrich, St. Louis, MO) for 4 and 24 h and supernatant levels of IL-8, IL1- α , TNF- α , IL-6, CXCL10 and CCL22 were analysed by multiplex assays using Milliplex (Millipore, Billerica, MA). Data were collected on the Bio-Plex flow cytometer (Bio-Rad, Hercules, CA).

2.8 | In vitro wound healing assays

Cells were seeded at a density of 100,000/well in 48-well plates. After overnight incubation, cells were transfected with mimetic, inhibitor or control as described above. After 24 h, a scratch was created using a sterile 1000 µl pipettor tip. Cells were monitored over 48 h and images captured on an Evos microscope (ThermoFisher Scientific, Waltham, MA) at 10 \times magnification. After assay incubation, cells were washed thrice with phosphate buffered saline (PBS), fixed with 2% paraformaldehyde and stained with haematoxylin and eosin.

2.9 | Flow cytometry

Intracellular expression of PLCB1 was assessed by flow cytometry and analysis performed using FlowJo software (Tree Star, Ashland, OR) as previously described (Naqvi et al., 2018a, 2018b) and detailed in Supplemental Materials and Methods.

2.10 | Phalloidin staining and image analysis

After 36 h, miR-26a-5p mimetic, inhibitor or control mimetic transfected cells were rinsed in PBS and fixed for 15 min in 4% paraformaldehyde/PBS. Samples were subsequently washed thrice and stained with rhodamine phalloidin (Molecular Probes, Eugene, OR) per manufacturer's instruction. Cells were washed with PBS and stained with Hoechst nuclear dye (Molecular Probes). Fluorescence images were captured using the Evos microscope at 20 \times magnification.

2.11 | Viability assays

Cell viability and proliferation was determined using the CellTiter 96 Aqueous Cell Proliferation Assay Kit (Promega, Madison, WI), flow cytometry and the LIVE/DEAD Fixable Violet Dead Cell

staining kit (Life Technologies), as previously described (Fordham et al., 2015).

2.12 | Western blot

Healthy and diseased gingival biopsies ($N = 3/\text{group}$) were collected, washed in sterile PBS and kept in $1\times$ lysis buffer with protease inhibitor cocktail until further use. Western blot was performed using PLCB1 and glyceraldehyde 3-phosphate dehydrogenase antibodies (both from Abcam, Cambridge, MA) as previously described (Naqvi et al., 2015; Valverde et al., 2020).

2.13 | Statistical analysis

Statistical analyses are described in detail in Supplemental Materials and Methods. Descriptive statistics and Cohort 1 data were analysed using GraphPad Prism (GraphPad Software, La Jolla, CA); analysis for Cohort 2 was conducted using SAS Statistical software (v. 9.4, SAS Institute, Cary, NC). The results from in vitro experiments were presented as means \pm SD or \pm SEM from three independent replicates, and experiments were conducted at least three times. The p -values were calculated using a Student's t -test and/or analysis of variance for more than two groups. A p -value $<.05$ was considered significant.

3 | RESULTS

3.1 | Decreased expression of miR-26a-5p and miR-26b-5p in periodontitis and its restoration after non-surgical therapy

To investigate whether miR-26 is responsive to therapy, we compared the expression of miR-26 isoforms (miR-26a-5p and miR-26b-5p) in gingiva collected from two geographically distinct cohorts. From Cohort 1, gingival biopsies were collected from periodontally healthy and diseased subjects prior to periodontal therapy. From Cohort 2, gingiva was collected from periodontally healthy subjects and from periodontitis subjects before and after scaling and root planing (4–6 weeks post-treatment). No differences in age or gender distribution were noted between the cohorts, although statistically significant differences in clinical parameters were evident post-SRP. As expected, PPD and BOP were significantly lower in the healthy group and in periodontitis subjects after SRP compared with baseline (Tables S1 and S2). In Cohort 1, quantitative PCR results showed significant downregulation of miR-26a-5p (fold change = 0.38 ± 0.14 ; Ct = 27.5 ± 3.12 ; $p <.05$) and miR-26b-5p (fold change = 0.41 ± 0.21 ; Ct = 29.6 ± 2.9 ; $p <.01$) in diseased biopsy specimens compared with healthy controls (miR-26a-5p Ct = 25 ± 2.5 ; miR-26b-5p Ct = 29.6 ± 2.9) (Figure 1a,b). Significantly reduced levels of miR-

26a-5p (fold change = 0.76 ± 0.55 ; Ct = 28.2 ± 2.75 ; $p <.05$) and miR-26b-5p (fold change = 0.44 ± 0.23 ; Ct = 28.5 ± 1.5 ; $p <.01$) were observed in diseased gingiva collected in Cohort 2, compared with healthy controls (miR-26a-5p Ct = 26 ± 3.8 ; miR-26b-5p Ct = 27.9 ± 1.9) (Figure 1c,d). Interestingly, the levels of miR-26a-5p (fold change = 2.1 ± 0.4 ; Ct = 25.6 ± 2.1 ; $p <.05$) and miR-26b-5p (fold change = 1.96 ± 0.59 ; Ct = 25.9 ± 1.5 ; $p <.01$) were significantly increased in gingival biopsies collected 4–6 weeks post-therapy compared with pre-treatment (Cohort 2) and were similar to levels observed in the healthy cohort (Figure 1c,d). Results from Cohort 2 show that miR-26 family was downregulated in diseased gingiva and its expression restored after periodontal therapy.

Next, we asked if miR-26 expression is responsive to periodontal therapy. Interestingly, levels of both miR-26a-5p and miR-26b-5p negatively correlated with PPD in the periodontitis and post-therapy groups, revealing a significant inverse correlation (for miR-26a-5p: $r = -0.82$, $p <.001$; for miR-26b-5p: $r = -0.78$, $p <.001$) (Figure 1e, f). Similarly, reduction in BOP post-therapy significantly correlated with an increase in miR-26a-5p ($r = -0.84$, $p <.001$) and miR-26b-5p ($r = -0.89$, $p <.001$). Overall, these findings strongly support that miR-26a-5p and -26b-5p levels respond to periodontal therapy and correlate with clinical parameters.

3.2 | Bioinformatic analysis reveals miR-26a-5p regulates pathways relevant to cytoskeletal organization, cell motility and innate immune responses

To test our hypothesis that miR-26a-5p plays an important role in the pathophysiology of periodontitis, we examined the underlying mechanism through which it could regulate the disease process by performing global pathway analysis using DIANA mirPath v.3 software. Our analysis identified several pathways associated with cytoskeletal organization, cell migration, immune cell development, cytokine signalling, etc. (Figure 2a). Pathway analysis predicted multiple gene targets of miR-26a-5p including PLCB1, a membrane-associated protein with key roles in intracellular signal transduction pathways associated with cytoskeletal reorganization and cell movement (Figure 2a).

3.3 | PLCB1 is a novel direct target of miR-26a-5p

Using a miRNA-target prediction tool (<http://mirwalk.umm.uni-heidelberg.de/>), we scanned the 3'UTR of PLCB1 for miR-26a/b binding sites. Three putative binding sites were identified for miR-26a-5p spread across the 3'UTR starting at nucleotide positions 620, 2398 and 2755, while two sites were identified for miR-26b-5p at positions 641 and 2659. Due to a long 3'UTR sequence and same seed sequence of miR-26a-5p and miR-26b-5p, we focused on the region that encompasses two binding sites for miR-26a-5p (2398, 2755). Further, we screened two additional miRNAs, miR-

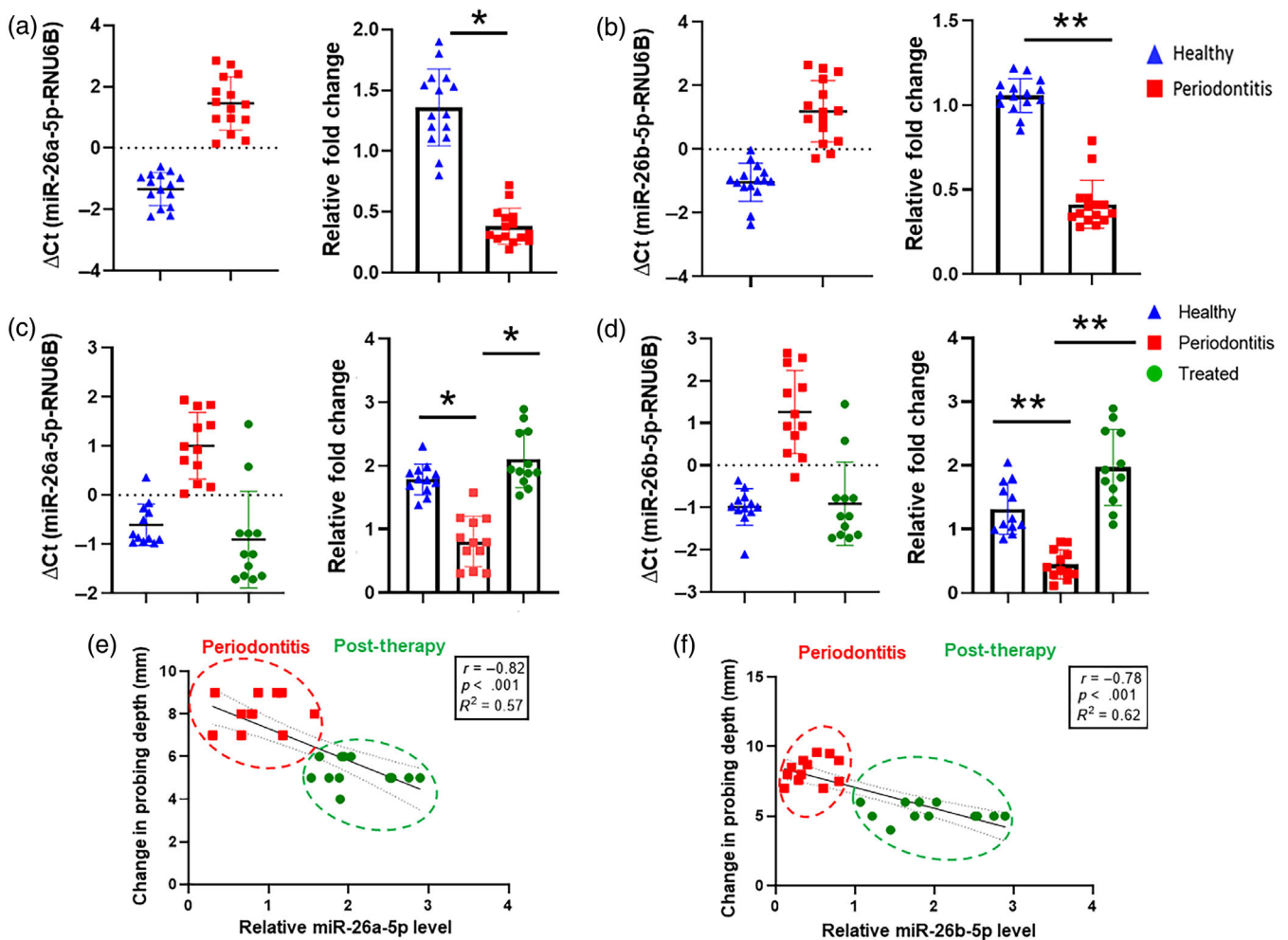


FIGURE 1 Downregulation of miR-26 family levels in gingival biopsies from periodontitis subjects and its restoration after therapy. (a) Quantitative PCR analysis of miR-26a-5p or (b) miR-26b-5p expression level in gingival biopsy samples of periodontitis patients ($N = 15$) as compared with those of healthy controls ($N = 15$) from Cohort 1, with histograms showing relative fold change expression of miR-26a-5p and miR-26b-5p, in periodontal inflamed and healthy gingiva. (c) Quantitative RT-PCR expression of miR-26a-5p, or (d) expression levels of miR-26b-5p in diseased gingival biopsy samples at baseline ($N = 12$) and 6 weeks post-therapy ($N = 12$) as compared with healthy controls ($N = 12$) from Cohort 2 with histogram showing relative fold change expression of miR-26a-5p and miR-26b-5p, in periodontal inflamed, treated and healthy gingiva. Results are normalized to those of controls and are represented relative to expression of the small nuclear RNA, RNU48. Student's *t*-test was used to calculate *p*-values. * $p < .05$. Data are presented as mean \pm SEM of three independent experiments. Expression of (e) miR-26a-5p and (f) miR-26b-5p negatively correlates with periodontal probing depth as measured in mm, in the periodontitis groups (pre- and post-therapy). ** $p < 0.01$

miR-101a-3p and miR-548a-3p, dysregulated in periodontal disease (Lee et al., 2011; Naqvi et al., 2019) and predicted to target the 3'UTR of PLCB1. Figure 2b and Figure S2A show sequence alignments of miR-26a-5p, miR-26b-5p, miR-101a-3p and miR-548-3p with the PLCB1 3'UTR in the cloned region. This was cloned downstream to the luciferase reporter and expression examined in the presence of miR-26a-5p, miR-101a-3p, miR-548a-3p mimetics or control mimetic. Compared with control mimetic, miR-26a-5p transfected cells, but not miR-101a-3p or miR-548a-3p transfected cells, exhibit reduced luciferase reporter activity (Figure 2c and Figure S2B), suggesting that the PLCB1 3'UTR has bona fide binding sites for miR-26a-5p.

3.4 | Upregulation of PLCB1 in periodontally diseased gingiva

To assess the functional interaction of miR-26a-5p and its target PLCB1 *ex vivo*, we examined PLCB1 mRNA and protein expression in gingival biopsies. In contrast to the downregulation of miR-26a-5p previously observed, we found upregulation of PLCB1 mRNA in diseased specimens (fold change = 3.41 ± 1.44 ; Ct = 29 ± 1.55 ; $p < .01$) compared with healthy controls (Ct = 32 ± 0.7 ; $p < .01$) as quantified by RT-qPCR (Figure 3a) and three-fold upregulation of PLCB1 protein in diseased samples by western blot (Figure 3b). In Cohort 2, a similar upregulation in PLCB1 mRNA was observed in periodontally diseased

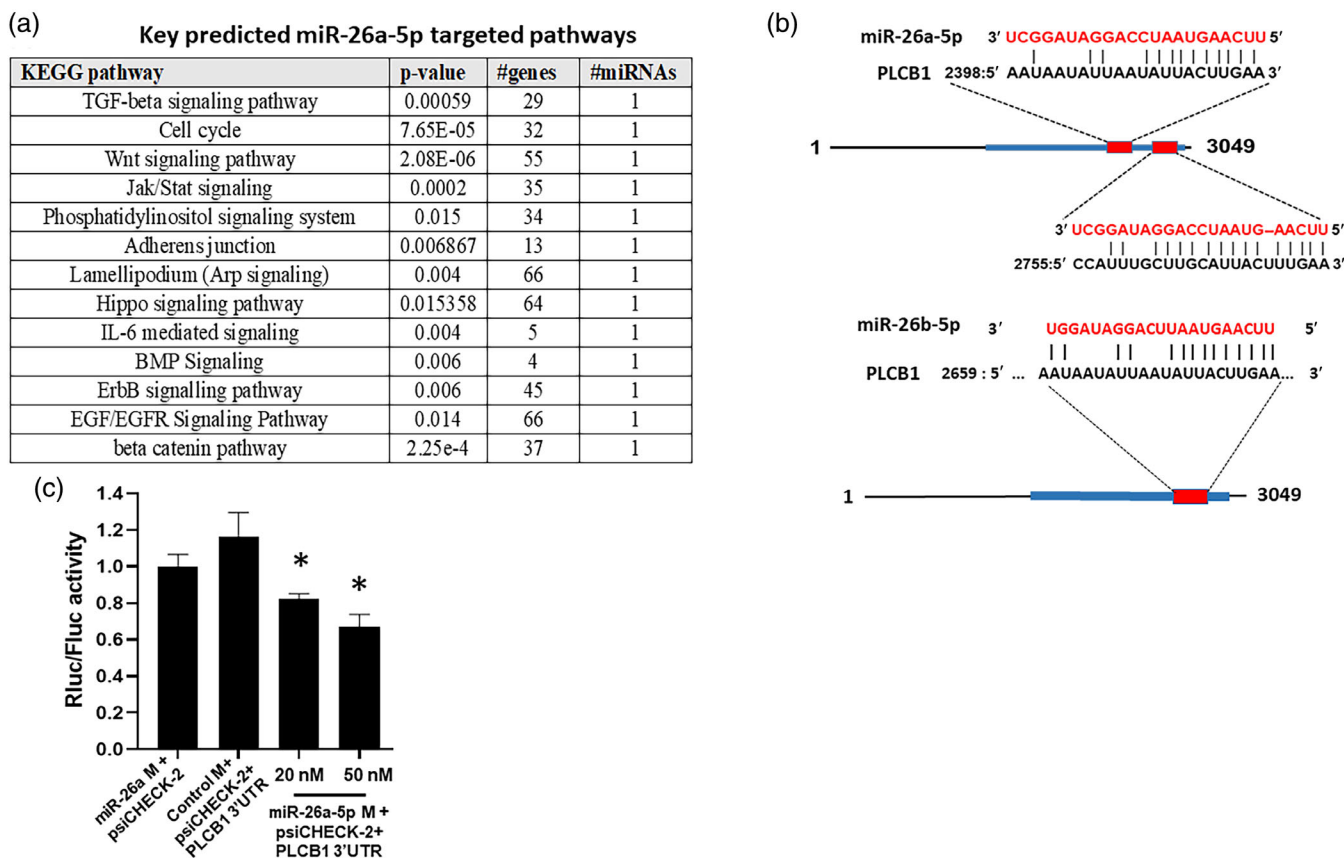


FIGURE 2 Phospholipase C beta 1 (PLCB1) is a novel direct target of miR-26a-5p. (a) Key predicted miR-26a-5p targeted pathways. (b) Sequence alignment of predicted miR-26a-5p and miR-26b-5p (red boxes) binding sites in the 3'UTR of human PLCB1. Blue line represents the cloned part of the entire PLCB1 3'UTR. (c) HEK293 cells were co-transfected with PLCB1 3'UTR construct and miR-26a-5p or control mimetic. Renilla activity was normalized to firefly activity, and the ratios subsequently normalized to empty vector transfected cells with miR-26a-5p mimetic set as 1. Data are expressed as mean \pm SEM of three independent transfections. * $p < .05$. M, mimetic

(fold change = 2.5 ± 0.51 ; Ct = 29 ± 0.55 ; $p < .05$) gingival samples compared with healthy group (Ct = 30.9 ± 0.7 ; Figure 3c). Conversely, periodontal therapy downregulated (fold change = 0.84 ± 0.48 ; Ct = 32 ± 1.9 ; $p < .01$) PLCB1 mRNA expression to levels similar to healthy gingiva (Figure 3c). Importantly, the expression of miR-26a-5p negatively correlated with PLCB1 expression before and after therapy in the periodontitis group, revealing a significant inverse correlation ($r = -0.79$, $p < .01$) between the expression levels of miR-26a-5p and PLCB1 (Figure 3d).

To further substantiate the biological relevance of miR-26a-5p and its target PLCB1 in periodontal disease, we examined their expression in a murine model of ligature-induced periodontitis. We observed increased expression of PLCB1 and decreased miR-26a-5p levels with the progression of periodontal disease (Figure 3e,f) corroborating our human cohort data. In vivo results strongly suggest that downregulation of miR-26a-5p correlates with an upregulation of PLCB1.

To demonstrate the functional impact of miR-26a-5p on PLCB1 expression, we examined protein and mRNA levels of PLCB1 in miR-26a-5p overexpressing cells (HOK, HEK293 and HeLa) by flow

cytometry, immunofluorescent microscopy and RT-qPCR, respectively. Compared with control mimetic or control inhibitor, we observed reduced protein levels of PLCB1 in miR-26a-5p transfected cells (Figure 3g,i). In addition, silencing of PLCB1 transcript was detected in miR-26a-5p overexpressing cells indicating that miRNA binding causes transcript degradation (Figure 3h). Thus, the differential expression of miR-26a-5p in periodontally diseased tissues will likely perturb functional regulation of PLCB1.

3.5 | miR-26a-5p regulates cytokine profiles in response to periopathogens in human oral keratinocytes

To gain better insight into the inflammatory control of miR-26a-5p, we performed multiplex analysis of six different cytokines/chemokines (IL-8, IL1- α , TNF- α , IL-6, CXCL10 and CCL22). Our results show that compared with control mimetic, miR-26a-5p transfected HOKs challenged with live *Pg* or *Aa* (50, 100 or 250 MOI) exhibit remarkably different cytokine/chemokine profiles. We noted a dose-

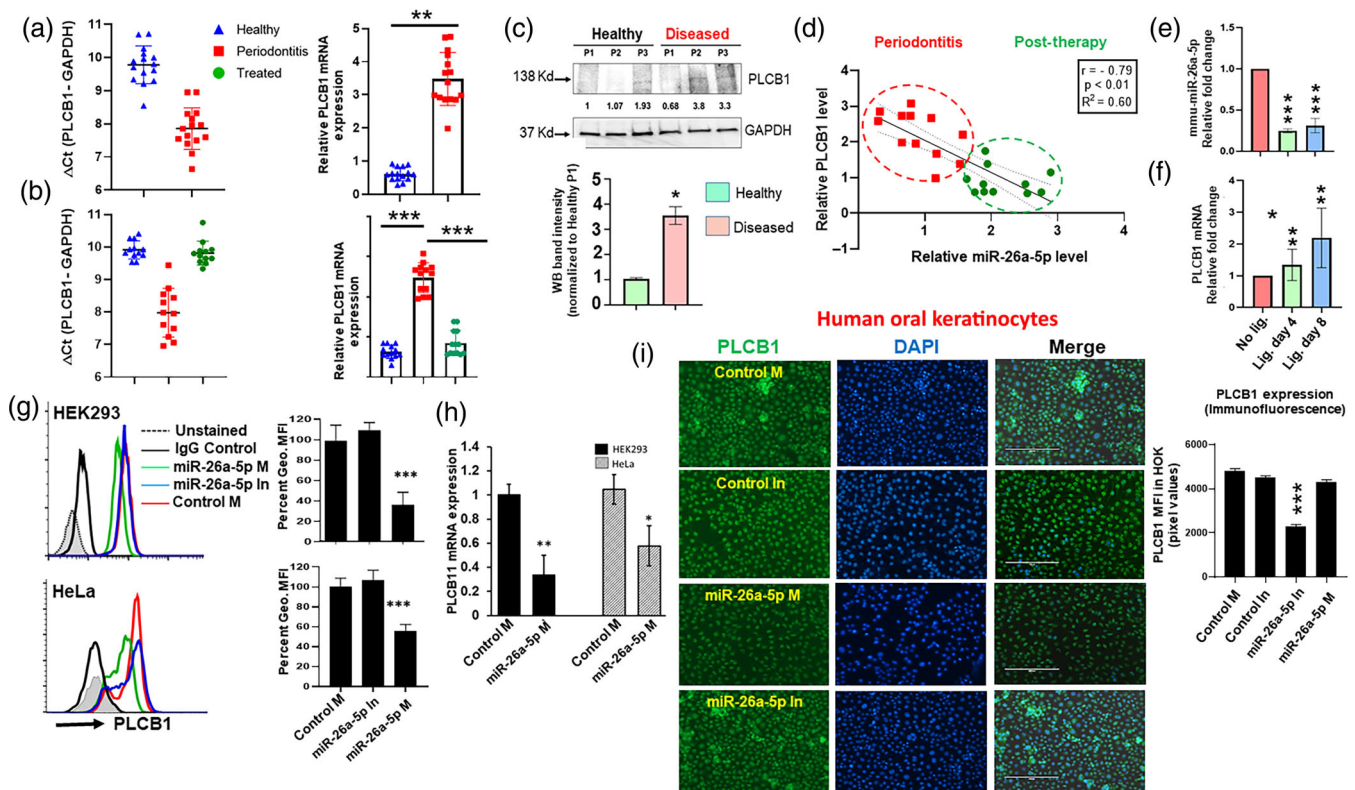


FIGURE 3 Upregulation of phospholipase C beta 1 (PLCB1) in periodontally diseased gingiva. (a) Quantitative PCR analysis of PLCB1 expression level in healthy and diseased gingival biopsy samples from Cohort 1 ($N = 15$ /group) with histograms showing relative expression of PLCB1. (b) Quantitative PCR analysis of PLCB1 expression of miR-26b-5p in diseased gingival biopsy samples at baseline ($N = 12$) and 4–6 weeks post-therapy ($N = 12$) as compared with healthy controls ($N = 12$) from Cohort 2. Results are normalized to those of controls and are represented relative to expression of glyceraldehyde 3-phosphate dehydrogenase (GAPDH). (c) Periodontally healthy and diseased gingival biopsies used for western blot analysis using PLCB1 and GAPDH antibodies. Histogram shows band intensities normalized to healthy sample P1. (d) Expression of miR-26a-5p negatively correlates with PLCB1 expression in the periodontitis patient groups (pre- and post-therapy). Relative expression of (e) miR-26a-5p and (f) PLCB1 quantified by RT-qPCR during disease progression (Day 4 and Day 8) in a murine model of ligature-induced periodontitis ($N = 3$ /time point). RNU6B and β -actin were used as endogenous controls for normalization. (g) HEK293 and HeLa cells transfected with miRNA mimetic, inhibitor or control were examined for PLCB1 protein levels by flow cytometry. Histograms show PLCB1 protein levels in cells. (h) Quantitative RT-PCR analysis of PLCB1 mRNA expression in miR-26a-5p or control mimetic transfected cells. Histograms showing relative fold change in HeLa and HEK293 cells. GAPDH was used as endogenous control. (i) HOK cells were transfected with miR-26a-5p mimetic, inhibitor or control mimetic and examined for protein levels of PLCB1 by immunostaining with anti-PLCB1 antibody. Nuclei were counterstained with Hoechst dye. Representative fluorescent images showing reduced intensity of PLCB1 levels in miR-26a-5p mimetic expressing oral keratinocyte cells compared with control and bar graph showing mean fluorescence intensity of PLCB1 on HOK cells in pixel units. Scale bar, 50 μ m. Arrows highlight differences in intensities of PLCB1 staining. Values are presented as mean \pm SD from three independent experiments. Student's t -test was used to calculate p -values. * $p < .05$; ** $p < .01$; *** $p < .001$; Student's t -test. In, inhibitor; M, mimetic

and time-dependent increase in cytokine levels in response to bacterial challenge. Specifically, compared with control mimetic, supernatant levels of IL-6, IL-8 and IL-1 α were significantly higher in miR-26a-5p mimetic-transfected cells challenged with live *Pg* or *Aa* (Figure 4a–h). At 4 h, only IL-8 showed significant increase in miR-26a-5p transfected cell challenged with 250 MOI of *Pg* (Figure 4a–c). At 24 h, IL-6 and IL-8 levels were significantly elevated in cultures challenged with *Pg* at all the MOI, while IL-1 α levels were elevated at 100 and 250 MOI (Figure 4a–c; summarized in Figure 4d).

In miR-26a-5p mimetic-transfected cells challenged with live *Aa*, we noted a significant upregulation of IL-8 after 4-h challenge at 50, 100 and 250 MOI (Figure 4f). At 24 h, IL-6 levels were

significantly higher at all the MOI and IL-8 levels were higher at 100 and 250 MOI, while supernatant levels of IL-1 α were significantly elevated at 250 MOI *Aa* challenge (Figure 4e–g; summarized in Figure 4h). CXCL10 did not show any significant difference at any time point or MOI (Figure S3C), while TNF- α and CCL22 were not detected at any of the time point examined for either *Pg* or *Aa* challenge at any time point or MOI challenge. These results suggest that immune modulation by miR-26a-5p was similar in both *Pg* and *Aa* challenged cells.

We also examined the impact of miR-26a-5p on cytokine/chemokine (same as listed in previous experiment) secretion by oral keratinocytes challenged with periodontopathogen-specific antigen,

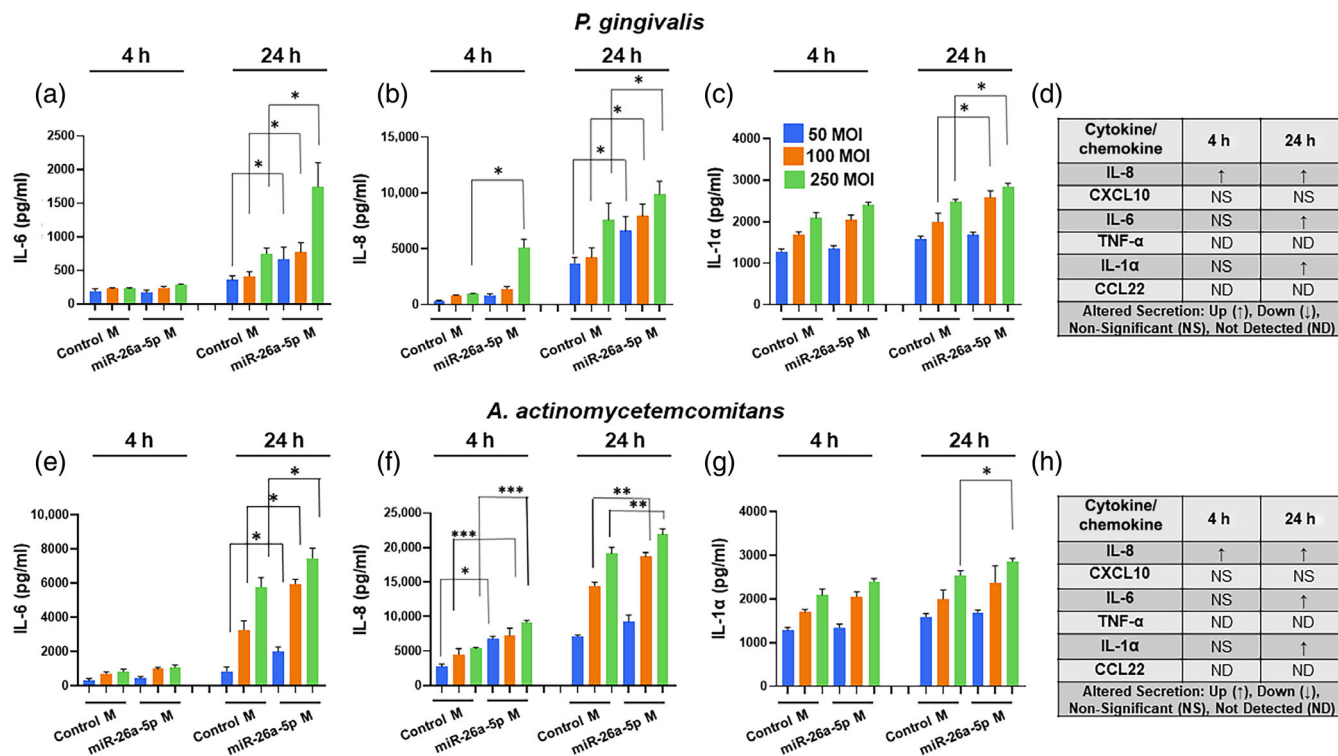


FIGURE 4 miR-26a-5p transfected cells secrete higher levels of cytokine/chemokines upon stimulation with live *Pg* or *Aa*. HOKs were transfected with miR-26a-5p or control mimetic. After 24 h, cells were challenged with either live *Porphyromonas gingivalis* at (a) 50 multiplicity of infection (MOI), (b) 200 MOI or (c) 500 MOI or live *Aggregatibacter actinomycetemcomitans* at (d) 50 MOI, (e) 200 MOI or (f) 500 MOI for 4 and 24 h and supernatants collected. Tables show a summary list of six different cytokines/chemokines analysed by multiplex bead array after 4 and 24 h challenge with live (g) *Pg* or (h) *Aa*. Data are presented as mean \pm SEM from four independent donors. Student's t-test was conducted to calculate *p*-values. **p* < .05; ***p* < .01; ****p* < .001. M, mimetic

Pg LPS. In HOK cells challenged with *Pg* LPS, IL-8 and CXCL10 supernatant levels were significantly elevated at both 4- and 24-h time points in cells transfected with miR-26a-5p compared with control mimetic, while IL-6 was elevated only at 24 h (Figure S3A,B). Interestingly, CCL22 levels were downregulated at 4 h before increasing at 24 h. TNF- α and IL-1 α were not detected at either time point. Together, these results show that higher levels of miR-26a-5p induces cytokine response against periodontal pathogens (live or their antigens) and dysregulation of miR-26a (as observed in PD) may impair immune response.

3.6 | Functional analysis identifies miR-26a-5p as a negative regulator of cell migration

We next examined the effects of miR-26a-5p on migration of HOK, HEK293 and HeLa cells. Cells transfected with miRNA or control mimetic were assayed for wound closure using a scratch assay over 48 h. Compared with control mimetic or mock transfected cells, miR-26a-5p transfected cells exhibit attenuated cell migration as observed by reduced wound closure (Figure 5a). Figure 5b shows average HOK cell count in the migration zone of cells expressing the indicated miRNA or control mimetic at 48 h post-scratch. Cells transfected with miR-26a-5p inhibitor demonstrated slightly increased migration, but

this was not significant. Further, in cells transfected with miR-26a-5p, migration was attenuated in a dose-dependent manner (20 and 50 nM) compared with control mimetic (Figure S4) at 24 h. Moreover, no significant changes in cell viability or proliferation were noted as assessed by 3-(4,5-dimethylthiazol-2-yl)-5-(3-carboxymethoxyphenyl)-2-(4-sulfophenyl)-2H-tetrazolium (MTS) assay and carboxyfluorescein succinimidyl ester staining in miR-26a-5p overexpressing cells, which negated the possibility that reduction in cellular migration was due to cell death or decreased proliferation (Figure 5c,d). These findings indicate that miR-26a-5p interferes with cell migration likely through direct targeting of its novel target PLCB1, thus supporting its specific role in regulating this key process. Importantly, using cell types not derived from oral tissues, our data suggest that the functional interaction between miR-26a-5p and its target PLCB1 can occur across tissues of various origins, thereby highlighting the functional importance of miR-26a-5p, a ubiquitously expressed miRNA.

3.7 | miR-26a-5p overexpressing cells display impaired cytoskeletal organization

The structure and shape of gingiva and periodontium as a whole are determined by the cellular molecular framework or cytoskeletal lattice. Cellular actin polymerization and disassembly play a crucial role

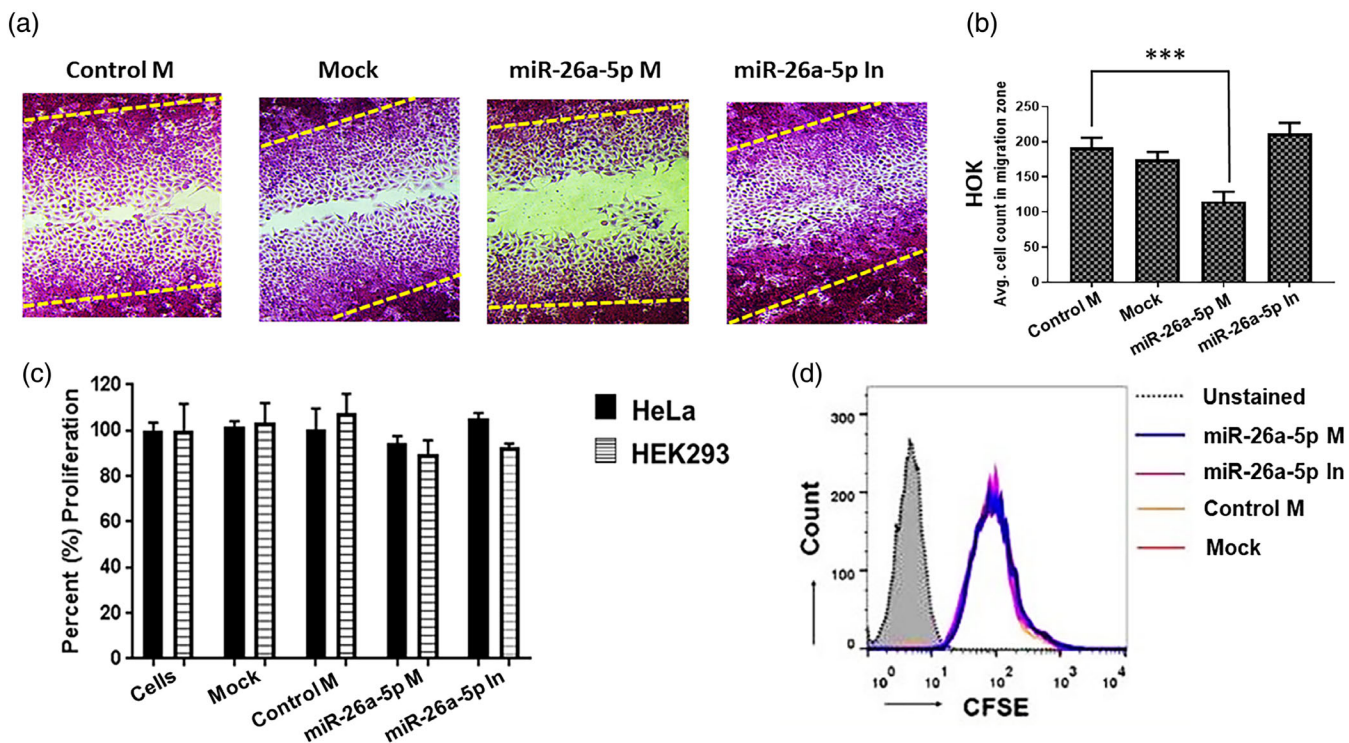


FIGURE 5 miR-26a-5p negatively regulates cell migration. Cultured HOK, HEK293 and HeLa cells were transfected with miRNA, inhibitor or control mimetic (all at 50 nM), and scratch wound healing assays were performed. (a) Representative image of HeLa cells were transfected with miR-26a-5p mimetic, inhibitor, control mimetic or mock (lipofectamine only) and wound closure assays performed at 48 h. H&E stained images of cells captured at the end of assay. Experiments were performed at least thrice with duplicate transfections. Bar—100 μ m. (b) Representative histogram of average HOK cell count in the migration zone at 24 h post-transfection with indicated miRNA mimetics or control. Reduced wound closure was noticed in miR-26a-5p compared with control mimetic. Experiments were performed at least thrice with duplicate transfections. (c) miR-26a-5p mimetic (M), inhibitor (In) or control mimetic transfected (all at 50 nM final concentration) HeLa and HEK293 cultures were assessed for cell viability using the 3-(4,5-dimethylthiazol-2-yl)-5-(3-carboxymethoxyphenyl)-2-(4-sulfophenyl)-2H-tetrazolium (MTS) assay. Histograms showing the similar viability in all transfected and mock samples. Values are presented as mean \pm SD from three independent experiments. No significant differences were observed in the cell viability. Student's *t*-test. (d) HeLa stained with carboxyfluorescein succinimidyl ester (CFSE) were transfected with miR-26a-5p mimetic (M), inhibitor (In) or control mimetic (M). Cell proliferation was assessed by examining CFSE fluorescence using flow cytometry. Histograms showing comparison of cell proliferation in transfected cells. The peaks in each histogram represent successive generations of live proliferating cells. All the treatments showed similar cell proliferation activity. **p* < .05; ***p* < .01; ****p* < .001; Student's *t*-test. HOK, human oral keratinocytes

in multiple diseases (Friedl & Gilmour, 2009). miR-26a-5p pathway analysis revealed multiple pathways related to cytoskeletal regulation. We therefore questioned whether miR-26a-5p mediated inhibition of cell migration is a result of aberrant actin polymerization. Cells transfected with miR-26a-5p mimetic, inhibitor or control were assessed for F-actin in two key cell types of the periodontium namely, HOK and PDL-F. Compared with inhibitor and control, lower concentration of F-actin staining was observed in miR-26a-5p mimetic expressing cells using immunofluorescent microscopy (Figure 6a,b). Conversely, miR-26a-5p inhibitor transfected HeLa cells exhibit long, bright and highly dense distribution of F-actin (Figure 6c) strongly supporting a role of miR-26a-5p in controlling the cytoskeletal network. These findings verify the functional interaction between miR-26a-5p and its PLCB1 in different cell types. Together, these results demonstrate miR-26a-5p can modulate actin organization, which in turn impairs cell migration.

4 | DISCUSSION

Disruption in cellular signal transduction pathways resulting from aberrations in miRNA expression may confer frequent and selective biological advantages during the propagation of periodontal disease (Perri et al., 2012; Pettiette et al., 2019; Naqvi & Slots, 2021), thereby leading to accelerated disease progression or delayed resolution. In order to correlate the observation of downregulated miR-26a-5p expression with the pathophysiology of periodontitis, we questioned its possible functional role in the disease process. Previously validated gene targets for miR-26a-5p including enhancer of zeste homologue 2 (EZH2), la-related protein 1 (LARP1) and transmembrane protein 184B (TMEM18) inhibit cell migration, proliferation and invasion, suggesting that miR-26a-5p may modulate cell survival through regulation of multiple pathways (Lu et al., 2011; Fukumoto et al., 2015; Kato et al., 2015). Conversely, miR-26a-5p overexpression is reported to promote cell

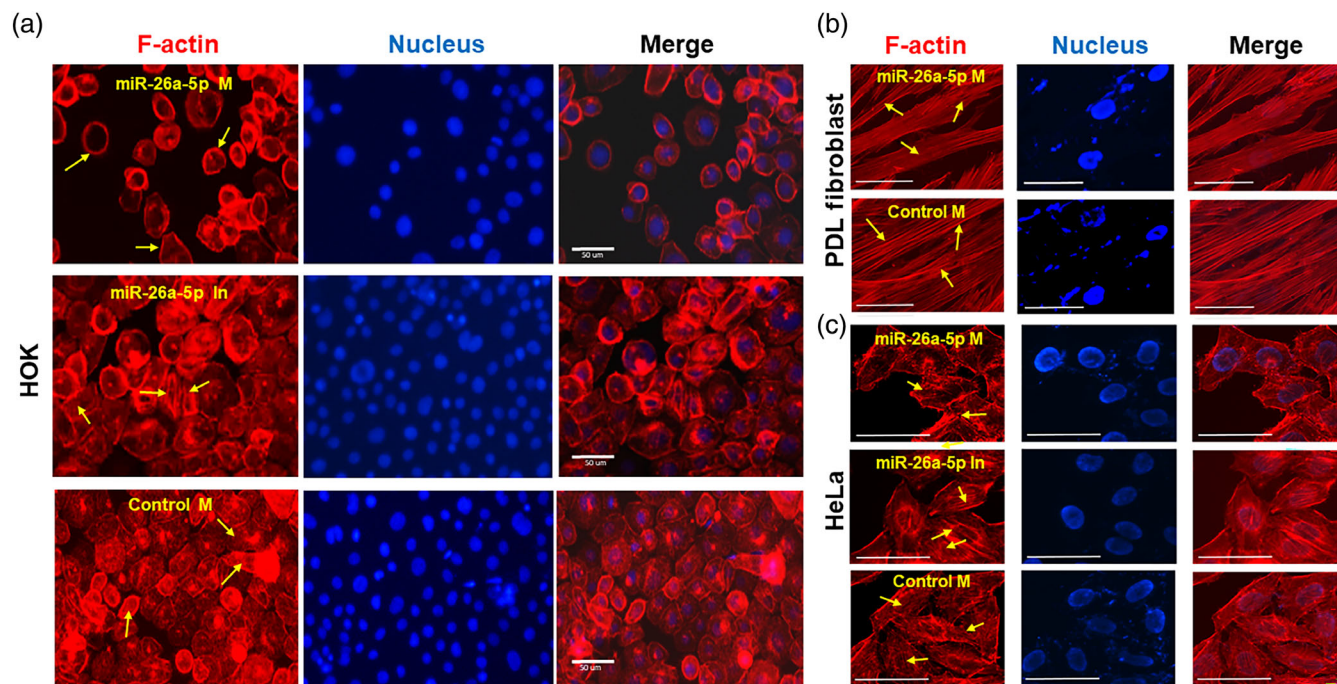
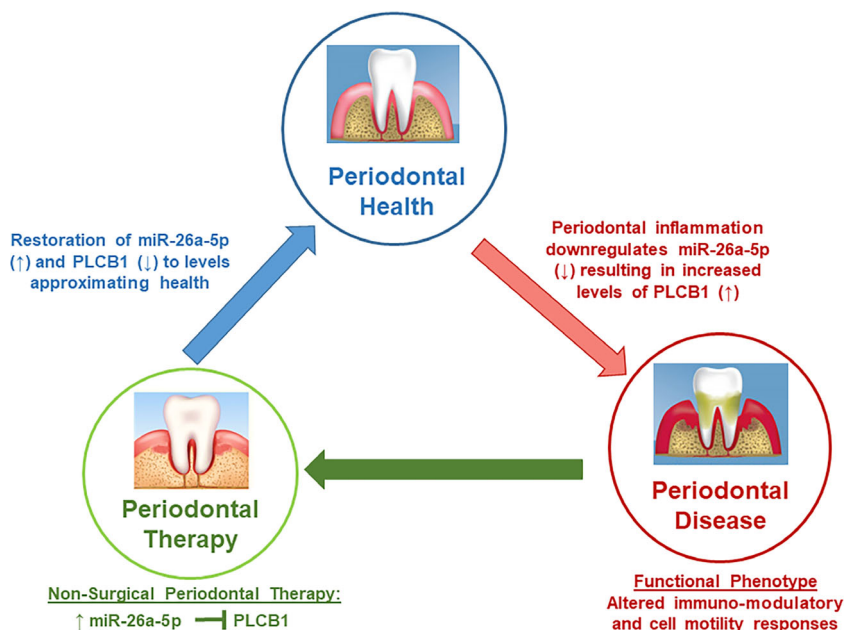


FIGURE 6 miR-26a-5p interferes with cytoskeletal organization and polymerization. (a) HOK, (b) periodontal ligament fibroblasts (PDL) fibroblasts and (c) HeLa cells were transfected with miR-26a-5p mimetic, inhibitor, control mimetic or control inhibitor and examined for F-actin organization by staining with rhodamine labelled phalloidin after 48 h. Nuclei were counterstained with Hoechst dye. Representative fluorescent images showing reduced F-actin intensity and organization in miR-26a-5p mimetic expressing HOK, PDL fibroblast and HeLa cells compared with control. Experiments were performed twice in triplicates with similar results. Scale bar, 50 μ m. Arrows highlight differences in actin fibre staining. HOK, human oral keratinocytes; PDL, periodontal ligament cells

FIGURE 7 Model illustrating the putative role of miR-26a-5p in periodontal health and disease. Downregulation of miR-26-5p in periodontitis can result in upregulation of phospholipase C beta 1 (PLCB1) and augmented cytokine/chemokine expression as seen by in vitro periodontitis model. Likewise, increased PLCB1 levels could promote cell migration as evidenced by the opposing effect in vitro with miR-26a-5p overexpression causing impaired cell migration/disorganized cytoskeleton in oral keratinocytes and PDL fibroblasts. After 4–6 weeks non-surgical periodontal therapy, miR-26a-5p levels are restored to levels approximating to those seen in periodontally healthy gingiva with a converse downregulated PLCB1 expression.



death by targeting anti-apoptotic genes such as induced myeloid leukaemia cell differentiation protein (Gao et al., 2013). Our results show that miR-26a-5p and its cognate target PLCB1 exhibit antagonistic relationship in gingival tissues derived from two independent cohorts of healthy and periodontally disease subjects, both at the RNA and protein levels. Importantly, miR-26a-5p levels exhibit significant correlation with

probing depth, BOP and PLCB1 in pre- and post-therapy subjects, strongly suggesting its role in disease progression and resolution. miR-26a-5p downregulation and induction of PLCB1 expression was also observed in a murine model of ligature-induced periodontitis, further supporting a key association between miRNA:mRNA expression and disease progression. Our dual luciferase assays show that miR-26a-5p

directly regulates PLCB1 by interacting with its 3'UTR and likely causes degradation of PLCB1 transcripts as observed by RT-qPCR in miR-26a-5p transfected cells. Moreover, reduced PLCB1 protein levels were detected in miR-26a-5p expressing cells. Thus, we identified a novel target of miR-26a-5p critical in signal transduction that may be relevant to periodontopathogenesis.

The pleiotropic impact of downregulated miR-26a-5p and upregulated PLCB1 expression in periodontitis can perturb pathways involved in inflammation, cell motility and cytoskeletal framework. Indeed, we previously reported impaired cell migration and structural defects in myeloid cells overexpressing miR-30b and miR-142-3p (Valverde et al., 2020). In this study, we show an immuno-modulatory role of miR-26a-5p in TLR-induced innate immune responses by enhancing cytokine/chemokine expression in miR-26a-5p transfected HOK challenged with live periodontopathogens or their LPS (Figure S3A,B). The observation of reduced miR-26a-5p and miR-26b-5p expression in diseased gingival tissues and restoration to levels comparable to healthy gingiva post-treatment ascertains the fact that miR-26 family members may be required for reinstating periodontal tissue homeostasis in inflammatory conditions and in modulating pro-inflammatory cytokine/chemokine levels. In addition, our results indicate marked changes in cytoskeletal organization in HOKs and PDL-F as observed by changes in F-actin staining patterns induced by miR-26a-5p mimetic. Decreased cellular migration upon enforced miR-26a-5p expression could be indicative of the possible requirement of a basal level of miR-26a-5p:PLCB1 in the active restructuring of periodontal tissues. Interestingly, suppressing the activity of miR-26a-5p by miRNA inhibitor relieves miR-26a-5p regulation of its target(s) and hence we noticed longer, intact and intensely stained actin fibres. Thus, miRNAs expressed in gingival tissues may actively participate in disease-associated tissue restructuring by directly targeting genes involved in cell migration of HOK and PDL-F, key cells of the periodontium.

Although our study did not determine the location of miR-26a-5p in periodontal tissues and cell components, the insights provided by our present data could pave the way for further analysis of miR-26a-5p in periodontal pathogenesis and resolution of inflammation. However, miR-26a-5p being ubiquitous is likely present in multiple cell types (Gao et al., 2013; Miyamoto et al., 2016). Extensive functional experiments in vitro, in animal models of periodontal disease along with studies with larger cohorts in humans, are required to validate the suitability of the miR-26a-5p for the development of potential biomarkers and therapeutic targets for periodontitis. This is especially important in validating expression of miR-26a-5p and PLCB1 in gingival specimens.

In conclusion, our results provide evidence of a significant role for miR-26a-5p in the regulation of diseases governed by host immune responses, such as periodontitis. The deranged immuno-modulatory and cell motility responses could occur via direct interaction with its target gene PLCB1, thereby affecting the biological functions and behaviour of cells. A noteworthy finding was that post-periodontal therapy, gingival levels of miR-26a-5p (and its gene target PLCB1) were restored to those observed in periodontally healthy subjects, further affirming

the role of miR-26a-5p in the periodontal tissue homeostasis (Figure 7). These results elucidate mechanisms whereby the inflammatory response and cell migration modulated by miR-26a-5p (and its interaction with PLCB1) can be potentially targeted for therapeutic purposes, thus unravelling the regulatory miRNA circuits and our understanding of immunobiology and periodontal pathology.

AUTHOR CONTRIBUTIONS

Juhi R. Uttamani, Afsar R. Naqvi, Varun Kulkarni and Salvador Nares conceived and designed the experiments. Juhi R. Uttamani, Afsar R. Naqvi, Araceli Maria Valverde Estepa, Varun Kulkarni, Maria F. Brambila, Gloria Martínez, Gabriela Chapa, Christine D. Wu and Wei Li performed the experiments. Juhi R. Uttamani, Afsar R. Naqvi, Sona Rivas-Tumanyan and Salvador Nares analysed the data. Juhi R. Uttamani, Afsar R. Naqvi and Salvador Nares wrote the paper.

ACKNOWLEDGEMENTS

We would like to thank Dr. Richard Lamont, University of Louisville, Louisville, Kentucky, USA and Dr. Xianghong Luan, Texas A&M University, Dallas, Texas, USA, for graciously providing the immortalized human gingival epithelial cell line and human periodontal ligament fibroblasts, respectively. We also thank Dr. Raza Ali Naqvi for his help with multiplex bead assay experiments.

FUNDING INFORMATION

This study was funded by Contract grant sponsor: NIDCR/NIH; contract grant numbers: DE021052 (SN), DE026259 (ARN) and DE027980 (ARN). Contract grant sponsor: UIC College of Dentistry; contract grant number: Edward C. Wach Fund.

CONFLICT OF INTEREST

All authors have read the manuscript and approved of the final version. The authors declare that the research was conducted in the absence of any conflicts of interest.

DATA AVAILABILITY STATEMENT

The data that support the findings of this study are available from the corresponding author upon reasonable request.

ETHICS STATEMENT

The study has been approved by the Institutional Review Boards of the University of Illinois Chicago (IRB approval #2105-1093) and University Autónoma de Nuevo León (IRB approval SPSI-010613).

ORCID

Salvador Nares  <https://orcid.org/0000-0002-2194-1374>

REFERENCES

- Fordham, J. B., Naqvi, A. R., & Nares, S. (2015). Regulation of miR-24, miR-30b, and miR-142-3p during macrophage and dendritic cell differentiation potentiates innate immunity. *Journal of Leukocyte Biology*, 98, 195–207.
- Friedl, P., & Gilmour, D. (2009). Collective cell migration in morphogenesis, regeneration and cancer. *Nature Reviews Molecular Cell Biology*, 10, 445–457.

- Fukumoto, I., Hanazawa, T., Kinoshita, T., Kikkawa, N., Koshizuka, K., Goto, Y., Nishikawa, R., Chiyomaru, T., Enokida, H., Nakagawa, M., Okamoto, Y., & Seki, N. (2015). MicroRNA expression signature of oral squamous cell carcinoma: Functional role of microRNA-26a/b in the modulation of novel cancer pathways. *British Journal of Cancer*, 112(5), 891–900.
- Gao, J., Li, L., Wu, M., Liu, M., Xie, X., Guo, J., Tang, H., & Xie, X. (2013). MiR-26a inhibits proliferation and migration of breast cancer through repression of MCL-1. *PLoS One*, 8(6), e65138.
- Guil, S., & Esteller, M. (2009). DNA methylomes, histone codes and miRNAs: Tying it all together. *International Journal of Biochemistry and Cell Biology*, 41, 87–95.
- Irimata, K., Paul, W., & Li, X. (2018). Estimation of correlation coefficient in data with repeated measures. SAS Global.
- Kato, M., Goto, Y., Matsushita, R., Kurozumi, A., Fukumoto, I., Nishikawa, R., Sakamoto, S., Enokida, H., Nakagawa, M., Ichikawa, T., & Seki, N. (2015). MicroRNA-26a/b directly regulate L-related protein 1 and inhibit cancer cell invasion in prostate cancer. *International Journal of Oncology*, 47(2), 710–718.
- Kulkarni, V., Naqvi, A. R., Uttamani, J. R., & Nares, S. (2016). MiRNA-target interaction reveals cell-specific post-transcriptional regulation in mammalian cell lines. *International Journal of Molecular Sciences*, 17, 72.
- Lee, Y. H., Na, H. S., Jeong, S. Y., Jeong, S. H., Park, H. R., & Chung, J. (2011). Comparison of inflammatory microRNA expression in healthy and periodontitis tissues. *Biocell*, 35(2), 43–49.
- Lu, J., He, M.-L., Wang, L., Chen, Y., Liu, X., Dong, Q., Chen, Y.-C., Peng, Y., Yao, K.-T., Kung, H.-F., & Li, X.-P. (2011). MiR-26a inhibits cell growth and tumorigenesis of nasopharyngeal carcinoma through repression of EZH2. *Cancer Research*, 71(1), 225–233.
- Miyamoto, K., Seki, N., Matsushita, R., Yonemori, M., Yoshino, H., Nakagawa, M., & Enokida, H. (2016). Tumour-suppressive miRNA-26a-5p and miR-26b-5p inhibit cell aggressiveness by regulating PLOD2 in bladder cancer. *British Journal of Cancer*, 115(3), 354–363.
- Naqvi, A. R., Brambila, M. F., Martínez, G., Chapa, G., & Nares, S. (2019). Dysregulation of human miRNAs and increased prevalence of HHV miRNAs in obese periodontitis subjects. *Journal of Clinical Periodontology*, 46, 51–61.
- Naqvi, A. R., Fordham, J. B., Khan, A., & Nares, S. (2014). MicroRNAs responsive to *Aggregatibacter actinomycetemcomitans* and *Porphyromonas gingivalis* LPS modulate expression of genes regulating innate immunity in human macrophages. *Innate Immunity*, 20, 540–551.
- Naqvi, A. R., Fordham, J. B., & Nares, S. (2015). miR-24, miR-30b and miR-142-3p regulate phagocytosis in myeloid inflammatory cells. *Journal of Immunology*, 194, 1916–1927.
- Naqvi, A. R., Shango, J., Seal, A., Shukla, D., & Nares, S. (2018a). Viral miRNAs alter host cell miRNA profiles and modulate innate immune responses. *Frontiers in Immunology*, 9, 433.
- Naqvi, A. R., Shango, J., Seal, A., Shukla, D., & Nares, S. (2018b). Herpesviruses and microRNAs: New pathogenesis factors in oral infection and disease? *Frontiers in Immunology*, 9, 2099.
- Naqvi, A. R., & Slots, J. (2021). Human and herpesvirus microRNAs in periodontal disease. *Periodontology 2000*, 87(1), 325–339.
- O'Connell, R. M., Rao, D. S., & Chaudhuri, A. A. (2010). Physiological and pathological roles for microRNAs in the immune system. *Nature Reviews Immunology*, 10, 111–122.
- Offenbacher, S., Barros, S. P., & Beck, J. D. (2008). Rethinking periodontal inflammation. *Journal of Periodontology*, 79, 1577–1584.
- Paraskevopoulou, M. D., Georgakilas, G., Kostoulas, N., Vlachos, I. S., Vergoulis, T., Reczko, M., Filippidis, C., Dalamagas, T., & Hatzigeorgiou, A. G. (2013). DIANA-microT web server v5.0: Service integration into miRNA functional analysis workflows. *Nucleic Acids Research*, 41(Web Server issue), W169–W173.
- Perri, R., Nares, S., & Zhang, S. (2012). MicroRNA modulation in obesity and periodontitis. *Journal of Dental Research*, 91(1), 33–38.
- Pettiette, M. T., Zhang, S., Moretti, A. J., Kim, S. J., Naqvi, A. R., & Nares, S. (2019). MicroRNA expression profiles in external cervical resorption. *Journal of Endodontics*, 45(9), 1106–1113.e2.
- Seo, J. Y., Park, Y. J., Yi, Y. A., Hwang, J. Y., Lee, I. B., Cho, B. H., Son, H. H., & Seo, D. G. (2015). Epigenetics: General characteristics and implications for oral health. *Restorative Dentistry & Endodontics*, 40, 14–22.
- Stoecklin-Wasmer, C., Guarnieri, P., & Celenti, R. (2012). MicroRNAs and their target genes in gingival tissues. *Journal of Dental Research*, 91, 934–940.
- Tonetti, M. S., Greenwell, H., & Kornman, K. S. (2018). Staging and grading of periodontitis: Framework and proposal of a new classification and case definition. *Journal of Periodontology*, 89(Suppl 1), S159–S172.
- Valverde, A., Nares, S., & Naqvi, A. R. (2020). Impaired cell migration and structural defects in myeloid cells overexpressing miR-30b and miR-142-3p. *Biochimica et Biophysica Acta - Gene Regulatory Mechanisms*, 1863, 194628.

SUPPORTING INFORMATION

Additional supporting information can be found online in the Supporting Information section at the end of this article.

How to cite this article: Uttamani, J. R., Naqvi, A. R., Estepa, A. M. V., Kulkarni, V., Brambila, M. F., Martínez, G., Chapa, G., Wu, C. D., Li, W., Rivas-Tumanyan, S., & Nares, S. (2023). Downregulation of miRNA-26 in chronic periodontitis interferes with innate immune responses and cell migration by targeting phospholipase C beta 1. *Journal of Clinical Periodontology*, 50(1), 102–113. <https://doi.org/10.1111/jcpe.13715>